Role of Reactive Oxygen Species (ROS) in the Regulation of Adipogenic Differentiation of Human Maxillary/Mandibular Bone Marrow-Derived Mesenchymal Stem Cells

Nao Ikeda, Masakazu Ishii*, Haruka Miyata, Yasuhiro Nishi, Fumio Suehiro, Naohiro Komabashiri, Tomoaki Sakurai, Masahiro Nishimura

Department of Oral and Maxillofacial Prosthodontics, Kagoshima University Graduate School of Medical and Dental Science, Kagoshima, 890-8544, Japan

***Corresponding author:**

Masakazu Ishii, PhD

Department of Oral and Maxillofacial Prosthodontics, Kagoshima University Graduate School of Medical and Dental Science, 8-35-1 Sakuragaoka, Kagoshima, 890-8544, Japan

E-mail: masai@dent.kagoshima-u.ac.jp

Acknowledgements

We thank Editage (www.editage.com) for English language proofing.

ABSTRACT

Background

Maxillary/mandibular bone marrow-derived mesenchymal stem cells (MBMSCs) exhibit a unique property of lower adipogenic potential than other bone marrow-derived MSCs. However, the molecular mechanisms regulating the adipogenesis of MBMSCs remain unclear. This study aimed to explore the roles of mitochondrial function and reactive oxygen species (ROS) in regulating the adipogenesis of MBMSCs.

Methods and Results

MBMSCs exhibited significantly lower lipid droplet formation than iliac BMSCs (IBMSCs). Moreover, the expression levels of CCAAT/enhancer-binding protein β (C/EBPβ), C/EBPδ, and early B cell factor 1 (Ebf-1), which are early adipogenic transcription factors, and those of peroxisome proliferator-activated receptor-γ (PPARγ) and C/EBPα, which are late adipogenic transcription factors, were downregulated in MBMSCs compared to those in IBMSCs. Adipogenic induction increased the mitochondrial membrane potential and mitochondrial biogenesis in MBMSCs and IBMSCs, with no significant difference between the two cell types; however, intracellular ROS production was significantly enhanced only in IBMSCs.

Furthermore, NAD(P)H oxidase 4 (NOX4) expression was significantly lower in MBMSCs than in IBMSCs. Increased ROS production in MBMSCs by NOX4 overexpression or treatment with menadione promoted the expression of early adipogenic transcription factors but did not induce that of late adipogenic transcription factors or lipid droplet accumulation.

Conclusions

These results suggest that ROS may be partially involved in the process of MBMSC adipogenic differentiation from undifferentiated cells to immature adipocytes. This study provides important insights into the tissue-specific properties of MBMSCs.

Keywords: mesenchymal stem cells, maxillary/mandibular bone, iliac bone, adipogenic differentiation, reactive oxygen species

Introduction

Mesenchymal stem cells (MSCs) are present in various tissues and can differentiate into mesoderm-derived tissues such as bones, cartilage, and fat [1-3]. Owing to differences in their embryological origin, MSCs exhibit different properties in different tissues [4-6]. We have previously reported the presence of MSCs in

the maxillary/mandibular bone marrow and that these cells (referred to as MBMSCs) scarcely differentiate into adipocytes [7]. Adipogenesis of MSCs is regulated by complex processes in which undifferentiated MSCs are committed to the adipocyte lineage (preadipocytes), and then preadipocytes differentiate into mature adipocytes [8]. CCAAT/enhancer-binding protein β (C/EBPβ), δ (C/EBPδ), and early B cell factor 1 (Ebf-1) are key transcription factors in the differentiation of undifferentiated MSCs into preadipocytes [9-12]. These transcription factors regulate the expression of peroxisome proliferator-activated receptor γ (PPARγ) and C/EBPα and initiate adipogenesis [9, 11, 12]. PPARγ and C/EBPα are critical transcription factors involved in the process of immature adipocytes into mature adipocytes by promoting the expression of various adipocyte metabolic factors [8]. However, the mechanisms by which the adipogenic potential of MBMSCs is suppressed have not been well reported.

Activation of mitochondrial function is critical for the regulation of stem cell differentiation; the induction of adipogenic differentiation shifts mitochondrial energy production from glycolysis to oxidative phosphorylation, resulting in the activation of mitochondrial function [13, 14]. The induction of adipogenesis increases mitochondrial membrane potential and biogenesis, which are important indicators of mitochondrial activity [14, 15]. In addition, the activation of mitochondrial function induces ATP production, thereby resulting in large amounts of reactive oxygen species (ROS), a byproduct of ATP production [16]. Excessive intracellular ROS causes cellular damage and dysfunction whereas controlled low basal ROS levels are necessary and beneficial to sustain cell functions [17]. Moreover, ROS play a role

in the regulation of adipogenesis; the knockdown of NAD(P)H oxidase 4 (Nox4) suppresses ROS production and adipogenesis in MSCs [18]. Furthermore, treatment with exogenous H_2O_2 promotes adipogenesis by increasing C/EBPβ and PPARγ expressions in 3T3-L1 preadipocytes [19]. However, the roles of mitochondrial function and ROS in the adipogenesis of MBMSCs remain unknown.

In the present study, we hypothesized that the low adipogenic capacity of MBMSCs may be due to suppressed mitochondrial function and ROS production during adipogenic differentiation. Therefore, we aimed to evaluate the differences in mitochondrial functional activation and ROS production during adipogenesis in MBMSCs and IBMSCs to reveal the underlying mechanisms of adipogenesis in MBMSCs.

Materials and methods

Isolation of MSCs from the maxillary/mandibular bone marrow

This study was approved by the Kagoshima University Hospital Clinical Research Ethics Committee (no.170263 EKI-KAI3). The bone marrow was isolated from the maxilla or mandible bone of five patients at the time of dental implant surgery using a previously reported method [20]. The collected bone marrow fluid was seeded in a cell culture dish, and the adhered and proliferated cells were used as MBMSCs.

Cell culture

Five IBMSCs (Lonza Group AG, Basel, Switzerland) were used in this study. MBMSCs and IBMSCs were cultured in an α-minimal essential medium (α-MEM) with 10% fetal bovine serum (FBS; Hyclone, Logan, UT, USA) and 1% Penicillin-Streptomycin Suspension (Life Technologies, Carlsbad, CA, USA) at 37 °C with 5% CO_2.

Adipogenic differentiation

Adipogenic differentiation was induced using an adipogenic induction medium [DMEM-high glucose supplemented with 10% FBS, 1% penicillin-streptomycin suspension, 1 μM dexamethasone (Dex), 0.5 mM 3-isobutyl-1-methyl-xanthine (IBMX), 0.2 mM indomethacin, and 10 μg/mL insulin] for 2 days, followed by culturing with adipogenic maintenance medium (DMEM-high glucose supplemented with 10% FBS, 1% penicillin-streptomycin suspension, and 10 μg/mL insulin) for another 2 days. In some experiments, adipogenic differentiation medium supplemented with 1000 nM menadione (2-methyl-1,4-naphthoquinone) (FUJIFILM Wako Pure Chemical Corp., Osaka, Japan) was used. Two weeks after adipogenic induction, lipid droplet formation was evaluated by Oil-Red-O staining. Formed lipid droplets were quantified by extracting the Oil-Red-O dye with 100% isopropyl alcohol and measuring the optical density at 540 nm with a microplate reader (Multiscan FC; Thermo Fisher Scientific, Waltham, MA, USA).

Photomicrographs were obtained using a phase contrast microscope (Olympus, Tokyo, Japan).

Quantitative real-time polymerase chain reaction (qRT- PCR) analysis

ISOGEN (Nippon Gene, Tokyo, Japan) was used for total RNA isolation. ReverTra Ace qPCR RT Master Mix (TOYOBO, Osaka, Japan) was used for reverse transcription of cDNA from isolated total RNA. mRNA expression levels were evaluated by qRT-PCR using the THUNDERBIRD SYBR Green PCR kit (TOYOBO) and CFX Connect Real-Time System (Bio-Rad Laboratories, Hercules, CA, USA). The sequences of the primers used in this study are listed in Supplementary Table 1.

Mitochondrial membrane potential analysis

Cells were cultured in Lab-TeK 8-well Chamber Slide (Thermo Fisher Scientific), and after reaching confluence, adipogenic induction was performed for 2 days. Cells were treated with a JC-1 solution (Dojindo, Kumamoto, Japan) at 37 °C for 30 min, washed with phosphate-buffered saline (PBS) (FUJIFILM Wako Pure Chemical Corp.), and photographed using a fluorescence microscope (Olympus, Tokyo, Japan). JC-1 dye accumulates and aggregates in the mitochondria depending on the mitochondrial membrane potential, resulting in a fluorescence shift from green to red. Quantitation of mitochondrial

membrane potential was assessed by measuring the ratio of red and green fluorescence using Image J software (National Institutes of Health, Bethesda, MD, USA).

Mitochondrial DNA (mtDNA) copy number analysis

Cells were cultured until confluence and then cultured in an adipogenic differentiation medium for 10 and 14 days. Total DNA was isolated using a NucleoSpin Tissue Kit (Macherey-Nagel, Düren, Germany) according to the manufacturer's instructions. Mitochondrial DNA copy number was assessed using the Human Mitochondrial DNA (mtDNA) Monitoring Primer Set (Takara Bio, Tokyo, Japan). NADH dehydrogenase subunit 1 (ND1) and solute carrier organic anion transporter family member 2B1 (SLCO2B1) were used to identify the mtDNA genome. Dehydrogenase subunit 5 (ND5) and serpin family A member 1 (SERPINA1) were used for genomic DNA detection. DNA amplification was performed using the THUNDERBIRD SYBR Green PCR kit (TOYOBO). The difference in the Ct values for the ND1/SLCO2B1 pair was calculated as follows: (ΔCt1 = Ct for SLCO2B1 – Ct for ND1) and ND5/SERPINA1 pair (ΔCt2 = Ct for SERPINA1 – Ct for ND5). The mtDNA copy number was calculated using the $2^{\Delta Ct}$ method.

NOX4 overexpression

MBMSCs were transfected with pCMV3-untagged-NOX4 vector or pCMV3-untagged Negative Control Vector (Sino Biological Inc., Beijing, China) by lipofectamine 2000 (Thermo Fisher Scientific) according to the manufacturer's instructions. Briefly, each plasmid was diluted with an Opti-MEM I reduced serum medium (Life Technologies) and then mixed with lipofectamine 2000 regent for 5 min. The mixture was added to MBMSCs and incubated for 6 h, and then the culture medium was replaced with a fresh medium. Cells were incubated for 2 days at 37 °C and 5% CO_2, for use in subsequent experiments.

Measurement of ROS levels

Cells seeded in 96-well black culture plates (Greiner Bio-One, Frickenhausen, Germany) were cultured until confluent and then subjected to adipogenic induction for 12 h, 24 h, 3 days, and 7 days. In some experiments, NOX4 plasmid vectors or control plasmid vectors were transfected after MBMSC seeding. Intracellular ROS levels were measured using the ROS Assay Kit-Highly Sensitive DCFH-DA (Dojindo). Cells were washed twice with Hanks' balanced salt solution (HBSS) (FUJIFILM Wako Pure Chemical Corp.) and then treated with a highly sensitive DCFH-dye solution at 37 °C for 30 min. The fluorescence intensity was measured using a TriStar^2 multimode plate reader (Berthold Technologies, Bad Wildbad, Germany). The total cell number in each well was measured using a Cell Count Normalization Kit (Dojindo). Cells were treated with the working solution supplied with the Kit for 30 min at 37 °C, after

which fluorescence intensity was measured using a TriStar2 multimode plate reader (Berthold Technologies). Intracellular ROS levels were normalized to the total cell number.

Cell viability assay

Cell viability assay was performed using the Premix WST-1 Cell Proliferation Assay System (Takara Bio). MBMSCs (1×10^3 cells) were seeded in 96-well cell culture plates and cultured until they adhered. Cells were then treated with 100–2000 nM menadione (FUJIFILM Wako Pure Chemical Corp.) or vehicle (dimethyl sulfoxide, DMSO) for 24, 48, or 72 h. Cells were incubated with Premix WST-1 at 37 °C for 40 min, and the absorbance was measured at 450 nm using a microplate reader (Multiscan FC; ThermoFisher Scientific).

Statistical analysis

The Shapiro–Wilk test was performed to assess the normality of data. For normally distributed data, Student's *t*-test was used for comparisons between two groups, and one-way analysis of variance with Tukey's post-hoc test was used for multiple comparisons. For non-normally distributed data, comparisons between two groups were performed using the Mann-Whitney U test, and multiple comparisons were

performed using the Kruskal–Wallis test, followed by the Dunn's–Bonferroni post-hoc test. Statistical significance was set as $p < 0.05$. All data analyses were performed using the SPSS software (version 28.0, SPSS Inc., Chicago, IL, USA).

Results

Comparison of the adipogenic potential of MBMSCs and IBMSCs

We first assessed cell surface antigen and stem cell marker expressions in undifferentiated MBMSCs and IBMSCs. The expression of cell surface antigen markers was similar between MBMSCs and IBMSCs (Supplementary Fig. 1A). The expression levels of Oct-4, SOX2, and Nanog, which are involved in the maintenance of MSC pluripotency [21], were comparable between undifferentiated MBMSCs and IBMSCs (Supplementary Fig. 1B). Next, we evaluated the adipogenic potential of MBMSCs and IBMSCs using Oil-Red-O staining, which showed that lipid droplet formation was significantly lower in MBMSCs than that in IBMSCs (Fig. 1A). We next investigated the expression of several adipogenesis-regulating transcription factors. C/EBPβ, C/EBPδ, and Ebf-1 are immediately induced after adipogenic differentiation and play important roles as initiators of adipogenesis [9-12]. We found that C/EBPβ, C/EBPδ, and Ebf-1 expression levels were significantly increased in IBMSCs at 24 h after adipogenic induction (Fig. 1B), whereas they were slightly, but not significantly increased, in MBMSCs (Fig. 1B). However, Ebf-1 expression levels in

MBMSCs were significantly lower than those in IBMSCs at 24 h after adipogenic induction (Fig. 1B). Next, we evaluated the expression levels of PPARγ and C/EBPα, which are essential transcription factors for the adipocyte maturation phase, and those of metabolic genes and adipokines. Adipogenic induction significantly promoted PPARγ and C/EBPα expression in IBMSCs, and their expression levels were significantly higher than those in MBMSCs (Fig. 1C). Adipogenic induction significantly increased the expression levels of LPL, aP2, and adiponectin expression in IBMSCs but not in MBMSCs (Fig. 1D). These results indicate that MBMSCs are negatively regulated at both the early and late stages of differentiation, which may contribute to the attenuation of lipid droplet formation.

Evaluation of mitochondrial function in MBMSCs and IBMSCs

We evaluated the mitochondrial membrane potential two days after adipogenic differentiation. Undifferentiated cells showed less accumulation of the JC-1 dye and emitted green fluorescence (Fig. 2A). Moreover, adipogenic induction increased the red fluorescence intensity of both IBMSCs and MBMSCs, and there was no significant difference in the increase in mitochondrial membrane potential between MBMSCs and IBMSCs (Fig. 2A). We also evaluated mitochondrial biogenesis during adipogenic induction in MBMSCs and IBMSCs and observed that adipogenic induction increased the mtDNA copy number in both IBMSCs and MBMSCs, with no significant difference between the two cell types at any time point

(Fig. 2B). Furthermore, we evaluated mitochondrial biogenesis-regulating gene expression. Adipogenic induction induced the expression of PGC-1α and TFAM in both MBMSCs and IBMSCs; however, there was no significant difference between the two cells (Fig. 2C). These results suggest that the activation of mitochondrial function is not directly involved in the adipogenic differentiation of MBMSCs.

Adipogenic differentiation induces intracellular ROS production in MBMSCs and IBMSCs

To investigate the involvement of ROS in the inhibition of adipogenesis in MBMSCs, we compared the intracellular ROS production levels during adipogenesis in MBMSCs and IBMSCs. ROS levels in IBMSCs, but not in MBMSCs, increased in a time-dependent manner (Fig. 3A). Because NOX4-derived ROS are important for the regulation of adipogenic differentiation [18], we investigated changes in NOX4 expression levels during adipogenic differentiation. In IBMSCs, NOX4 expression was temporarily reduced 24 h after adipogenic induction; however, on day 7, it was similar to that in undifferentiated cells (Fig. 3B). In contrast, NOX4 expression did not change following adipogenic induction in MBMSCs. Furthermore, NOX4 expression in MBMSCs was significantly lower than in IBMSCs at all time points (Fig. 3B). These results suggest that NOX4-derived ROS may be involved in the regulation of MBMSC adipogenesis.

Evaluation of the effect of increased ROS production by NOX4 overexpression on MBMSC adipogenesis

To further evaluate the involvement of NOX4-derived ROS in the MBMSC adipogenesis, NOX4 gene was overexpressed in MBMSCs. MBMSCs were transfected with pCMV3-negative control plasmid or pCMV3-NOX4 plasmid, and then NOX4 mRNA expression was evaluated. NOX4 mRNA expression level at day 3 after transfection was significantly higher in NOX4 plasmid-transfected cells than negative control plasmid-transfected cells (Fig. 4A). Furthermore, overexpression of NOX4 was confirmed to significantly increase ROS production in MBMSCs (Fig. 4B). Next, we evaluated the adipogenic potential of NOX4-overexpressing MBMSCs. First, we investigated the changes in the adipogenic transcription factors expression levels. C/EBPβ, C/EBPδ, and Ebf-1 expression in NOX4-overexpressing cells was higher than that of negative control plasmid transfected cells, and C/EBPδ in NOX4-overexpressing cells was significantly higher than in control cells (Fig. 4C). In contrast, there was no significant increase in PPARγ and C/EBPα expression in NOX4-overexpressing cells (Fig. 4D). MBMSCs transfected with pCMV3-negative control plasmid or pCMV3-NOX4 plasmid were subjected to adipogenic induction for 14 days, and then lipid droplet formation was evaluated. NOX4-overexpressing cells had no significant difference in lipid droplet formation compared to negative control plasmid-transfected cells (Fig. 4E). These results indicate that ROS induced by NOX4 overexpression may affect only early stages of adipose differentiation.

Evaluation of the effect of menadione-induced ROS on MBMSC adipogenesis

Menadione is a synthetic derivative of vitamin K and generates ROS via a one-electron reduction mechanism [22]. Therefore, we investigated the effect of menadione-induced intracellular ROS production on adipogenic differentiation of MBMSCs. We evaluated the cytotoxicity of menadione in MBMSCs and observed that treatment with menadione (100–1000 nM) for 72 h showed no cytotoxic effect whereas treatment with 2000 nM menadione showed cytotoxicity (Fig. 5A). Next, we evaluated the effects of treatment with menadione on ROS production. Treatment with menadione induced ROS production in MBMSCs, and 1000 nM of menadione significantly induced ROS production at all the evaluated time points (Fig. 5B). Therefore, 1000 nM was used in subsequent experiments. We then investigated the effect of the induction of intracellular ROS production on the adipogenic differentiation of MBMSCs. Menadione significantly increased C/EBPβ and C/EBPδ expression levels (Fig. 6A); however, no change was observed in PPARγ and C/EBPα expression levels (Fig. 6B). We evaluated the effects of ROS induction on lipid droplet formation and observed that treatment with menadione did not promote lipid droplet formation (Fig. 6C). These results indicate that ROS production induction by menadione treatment may affect only the early stages of adipogenic differentiation, similar to NOX4 gene overexpression.

Discussion

MSCs exhibit tissue-specific characteristics; MBMSCs have a lower adipogenic potential than other BMSCs. However, the reason why MBMSCs scarcely differentiate into adipocytes remains unknown. In this study, we demonstrated that ROS may be partially involved in the adipogenic differentiation process of MBMSCs.

Adipogenic differentiation of MSCs is mainly regulated in two stages: the determination and the terminal differentiation phases [8]. However, it is unclear at which phase stage MBMSC suppression occurs. In the present study, the expressions of C/EBPβ, C/EBPδ, and Ebf-1, which are early adipogenic transcription factors, were not increased in MBMSCs following adipogenic induction. C/EBPβ and C/EBPδ have been reported to induce adipogenic differentiation by regulating the expression of PPARγ and C/EBPα [9, 11]. As expected, PPARγ and C/EBPα expression levels in MBMSCs were significantly lower than those in IBMSCs. Therefore, the suppression of PPARγ and C/EBPα expression in MBMSCs may be C/EBPβ- and C/EBPδ-dependent. Ebf-1 induces adipogenic differentiation by directly binding to PPARγ and C/EBPα [12]. Furthermore, Ebf-1 expression is regulated by C/EBPβ and C/EBPδ [12]. Thus, low expression of C/EBPβ and C/EBPδ may have led to the suppression of Ebf-1 expression in MBMSCs. These results indicate that the negative regulation during the early adipogenic differentiation may be critical for MBMSC adipogenesis.

Several factors, including chemical, physical, and biological factors are crucial in the lineage commitment of MSCs [23]. Chemical factors such as Dex, IBMX, and indomethacin contained in the differentiation medium regulate differentiation by directly regulating transcription factor expression [24, 25]. Physical factors, such as mechanical force and the extracellular matrix, regulate differentiation through various intracellular signals [23]. Biological factors, such as cell metabolism, are closely involved in regulating MSC differentiation [23]. In particular, mitochondrial function and ROS generation are key regulators of adipogenic differentiation [13, 14, 18, 19]. In our study, the activation of mitochondrial function induced by adipogenic differentiation was comparable between MBMSCs and IBMSCs, suggesting that the activation of mitochondrial function may not be directly involved in the regulation of MBMSC adipogenesis.

The major sources of ROS are mitochondrial complexes I and III and NOX4 [26]. NOX4-derived ROS are important for the regulation of adipose differentiation. Treatment with antioxidant N-acetyl-L-cysteine or NOX4 siRNA suppresses the adipogenesis of the mouse mesenchymal stem cell line 10T1/2 [18]. Furthermore, NOX4 overexpression induces adipogenesis in 3T3-L1 preadipocytes and human adipose-derived MSCs [27, 28]. In the present study, NOX4 expression in MBMSCs was significantly lower than that in IBMSCs at all stages in undifferentiated and adipogenic differentiated cells. Furthermore, adipogenic induction promoted intracellular ROS production in IBMSCs but suppressed it in MBMSCs. These results indicate that NOX4-derived ROS may play a role in the regulation of MBMSC adipogenesis. Moreover,

NOX4 expression was suppressed in MBMSCs, even in undifferentiated cells; however, ROS production was similar between undifferentiated MBMSCs and IBMSCs. These results suggest that sources other than NOX4 may be important for ROS production in undifferentiated MBMSCs. Therefore, future studies should comprehensively investigate the mechanisms underlying the regulation of ROS production in MBMSCs.

In addition, we evaluated the effect of NOX4 gene overexpression on adipogenesis in MBMSCs to investigate the involvement of ROS in suppressing adipogenesis of MBMSCs. NOX4 overexpression induced intracellular ROS production and the expression of C/EBPβ, C/EBPδ, and Ebf-1 in MBMSCs. However, it did not significantly increase PPARγ and C/EBPα expression levels or lipid droplet accumulation. We also evaluated the effects of menadione-induced intracellular ROS on adipogenesis in MBMSCs. Treatment with menadione significantly enhanced the expression of C/EBPβ and C/EBPδ, but not the terminal differentiation of adipocytes. These results indicate that ROS may function as an early initiator of adipogenesis process. Consistent with our results, a previous study has shown that ROS production during 12–24 h of adipogenic induction is important for the promotion of adipogenesis [19]. Several studies have reported that increased ROS production promotes adipogenesis by inducing the expression and DNA-binding activity of C/EBPβ [29, 30]. However, it is unclear why adipocyte maturation was not induced in our study despite the upregulation of early adipogenic transcription factors. Previous studies reported that prolonged exposure to ROS suppresses insulin-induced lipogenesis and glucose uptake

in 3T3-L1 cells [31, 32]. It has also been reported that a transient increase in intracellular ROS is important for insulin signaling [33]. In the present study, we treated MBMSCs with menadione continuously for 14 days, and this continuously forced induction of ROS production may have had a suppressive effect on adipocyte maturation. Another study has shown that the induction of PPARγ transcription requires mitochondrial complex III-derived ROS [34]. In the present study, we only evaluated the effects of NOX4-derived ROS production on the adipogenic differentiation of MBMSCs. Therefore, future studies should investigate the effects of mitochondria-derived ROS on MBMSC adipogenesis.

In this study, ROS production patterns differed between MBMSCs and IBMSCs; however, the cause of this difference is unknown. MSCs retain the site-specific memories of the tissue of origin and the information about the physical environment that they have previously encountered, which influences cell fate [6, 35]. Differences in ROS production patterns between MBMSCs and IBMSCs may also be due to their developmental origins and localized microenvironments. In the future, the mechanism of ROS production in MBMSCs should be comprehensively investigated.

In conclusion, this study revealed that the suppression of the increased ROS production by adipogenic induction may cause low adipogenic potential in MBMSCs, providing important clues for elucidating the tissue-specific properties of MBMSCs.

Author contributions

Conceptualization: MI; methodology: NI and MI; data analysis and interpretation: NI, MI, HM, YN, FS, NK, and TS; writing-original draft preparation: NI, MI, and MN; funding acquisition: MI and MN. All the authors have read and approved the submission of this manuscript.

Funding

This work was supported in part by JSPS KAKENHI Grant Numbers JP20H03881 and JP21K10005.

Compliance with ethical standards

Competing interests

The authors have no relevant financial or non-financial interests to disclose.

Ethics approval

This study was conducted in accordance with the principles of the Declaration of Helsinki and approved by the Kagoshima University Hospital Clinical Research Committee, Kagoshima, Japan (no. 170263 EKI-KAI3).

Consent to participate

Written informed consent was obtained from all patients.

Consent to publish

The patients involved in this study provided informed consent for the publication of their data.

References

1. Pittenger MF, Mackay AM, Beck SC, Jaiswal RK, Douglas R, Mosca JD, Moorman MA, Simonetti DW, Craig S and Marshak DR (1999) Multilineage potential of adult human mesenchymal stem cells. Science 284:143-7. doi: 10.1126/science.284.5411.143

2. Lv FJ, Tuan RS, Cheung KM and Leung VY (2014) Concise review: the surface markers and identity of human mesenchymal stem cells. Stem Cells 32:1408-19. doi: 10.1002/stem.1681

3. Yin JY, Luo XH, Feng WQ, Miao SH, Ning TT, Lei Q, Jiang T and Ma DD (2021) Multidifferentiation potential of dental-derived stem cells. World J Stem Cells 13:342-365. doi: 10.4252/wjsc.v13.i5.342

4. Akintoye SO, Lam T, Shi S, Brahim J, Collins MT and Robey PG (2006) Skeletal site-specific characterization of orofacial and iliac crest human bone marrow stromal cells in same individuals. Bone

38:758-68. doi: 10.1016/j.bone.2005.10.027

5. Bugueno J, Li W, Salat P, Qin L and Akintoye SO (2017) The bone regenerative capacity of canine mesenchymal stem cells is regulated by site-specific multilineage differentiation. Oral Surg Oral Med Oral Pathol Oral Radiol 123:163-172. doi: 10.1016/j.oooo.2016.09.011

6. Onizuka S, Yamazaki Y, Park SJ, Sugimoto T, Sone Y, Sjoqvist S, Usui M, Takeda A, Nakai K, Nakashima K and Iwata T (2020) RNA-sequencing reveals positional memory of multipotent mesenchymal stromal cells from oral and maxillofacial tissue transcriptomes. BMC Genomics 21:417. doi: 10.1186/s12864-020-06825-2

7. Miyata H, Ishii M, Suehiro F, Komabashiri N, Ikeda N, Sakurai T and Nishimura M (2023) Elucidation of adipogenic differentiation regulatory mechanism in human maxillary/mandibular bone marrow-derived stem cells. Arch Oral Biol 146:105608. doi: 10.1016/j.archoralbio.2022.105608

8. Ambele MA, Dhanraj P, Giles R and Pepper MS (2020) Adipogenesis: A Complex Interplay of Multiple Molecular Determinants and Pathways. Int J Mol Sci 21. doi: 10.3390/ijms21124283

9. Hishida T, Nishizuka M, Osada S and Imagawa M (2009) The role of C/EBPdelta in the early stages of adipogenesis. Biochimie 91:654-7. doi: 10.1016/j.biochi.2009.02.002

10. Almalki SG and Agrawal DK (2016) Key transcription factors in the differentiation of mesenchymal stem cells. Differentiation 92:41-51. doi: 10.1016/j.diff.2016.02.005

11. Wu Z, Bucher NL and Farmer SR (1996) Induction of peroxisome proliferator-activated receptor

gamma during the conversion of 3T3 fibroblasts into adipocytes is mediated by C/EBPbeta, C/EBPdelta, and glucocorticoids. Mol Cell Biol 16:4128-36. doi: 10.1128/MCB.16.8.4128

12. Jimenez MA, Akerblad P, Sigvardsson M and Rosen ED (2007) Critical role for Ebf1 and Ebf2 in the adipogenic transcriptional cascade. Mol Cell Biol 27:743-57. doi: 10.1128/MCB.01557-06

13. Yan W, Diao S and Fan Z (2021) The role and mechanism of mitochondrial functions and energy metabolism in the function regulation of the mesenchymal stem cells. Stem Cell Res Ther 12:140. doi: 10.1186/s13287-021-02194-z

14. Hofmann AD, Beyer M, Krause-Buchholz U, Wobus M, Bornhauser M and Rodel G (2012) OXPHOS supercomplexes as a hallmark of the mitochondrial phenotype of adipogenic differentiated human MSCs. PLoS One 7:e35160. doi: 10.1371/journal.pone.0035160

15. Zhang Y, Marsboom G, Toth PT and Rehman J (2013) Mitochondrial respiration regulates adipogenic differentiation of human mesenchymal stem cells. PLoS One 8:e77077. doi: 10.1371/journal.pone.0077077

16. Xu X, Duan S, Yi F, Ocampo A, Liu GH and Izpisua Belmonte JC (2013) Mitochondrial regulation in pluripotent stem cells. Cell Metab 18:325-32. doi: 10.1016/j.cmet.2013.06.005

17. Zhang J, Xiang H, Liu J, Chen Y, He RR and Liu B (2020) Mitochondrial Sirtuin 3: New emerging biological function and therapeutic target. Theranostics 10:8315-8342. doi: 10.7150/thno.45922

18. Kanda Y, Hinata T, Kang SW and Watanabe Y (2011) Reactive oxygen species mediate adipocyte

differentiation in mesenchymal stem cells. Life Sci 89:250-8. doi: 10.1016/j.lfs.2011.06.007

19. Lee H, Lee YJ, Choi H, Ko EH and Kim JW (2009) Reactive oxygen species facilitate adipocyte differentiation by accelerating mitotic clonal expansion. J Biol Chem 284:10601-9. doi: 10.1074/jbc.M808742200

20. Suehiro F, Ishii M, Asahina I, Murata H and Nishimura M (2017) Low-serum culture with novel medium promotes maxillary/mandibular bone marrow stromal cell proliferation and osteogenic differentiation ability. Clin Oral Investig 21:2709-2719. doi: 10.1007/s00784-017-2073-7

21. Greco SJ, Liu K and Rameshwar P (2007) Functional similarities among genes regulated by OCT4 in human mesenchymal and embryonic stem cells. Stem Cells 25:3143-54. doi: 10.1634/stemcells.2007-0351

22. Funk MI, Conde MA, Piwien-Pilipuk G and Uranga RM (2021) Novel antiadipogenic effect of menadione in 3T3-L1 cells. Chem Biol Interact 343:109491. doi: 10.1016/j.cbi.2021.109491

23. Chen Q, Shou P, Zheng C, Jiang M, Cao G, Yang Q, Cao J, Xie N, Velletri T, Zhang X, Xu C, Zhang L, Yang H, Hou J, Wang Y and Shi Y (2016) Fate decision of mesenchymal stem cells: adipocytes or osteoblasts? Cell Death Differ 23:1128-39. doi: 10.1038/cdd.2015.168

24. Cao Z, Umek RM and McKnight SL (1991) Regulated expression of three C/EBP isoforms during adipose conversion of 3T3-L1 cells. Genes Dev 5:1538-52. doi: 10.1101/gad.5.9.1538

25. Lehmann JM, Lenhard JM, Oliver BB, Ringold GM and Kliewer SA (1997) Peroxisome

proliferator-activated receptors alpha and gamma are activated by indomethacin and other non-steroidal anti-inflammatory drugs. J Biol Chem 272:3406-10. doi: 10.1074/jbc.272.6.3406

26. Atashi F, Modarressi A and Pepper MS (2015) The role of reactive oxygen species in mesenchymal stem cell adipogenic and osteogenic differentiation: a review. Stem Cells Dev 24:1150-63. doi: 10.1089/scd.2014.0484

27. Schroder K, Wandzioch K, Helmcke I and Brandes RP (2009) Nox4 acts as a switch between differentiation and proliferation in preadipocytes. Arterioscler Thromb Vasc Biol 29:239-45. doi: 10.1161/ATVBAHA.108.174219

28. Higuchi M, Dusting GJ, Peshavariya H, Jiang F, Hsiao ST, Chan EC and Liu GS (2013) Differentiation of human adipose-derived stem cells into fat involves reactive oxygen species and Forkhead box O1 mediated upregulation of antioxidant enzymes. Stem Cells Dev 22:878-88. doi: 10.1089/scd.2012.0306

29. Chen X, Zhao C, Xu Y, Huang K, Wang Y, Wang X, Zhou X, Pang W, Yang G and Yu T (2021) Adipose-specific BMP and activin membrane-bound inhibitor (BAMBI) deletion promotes adipogenesis by accelerating ROS production. J Biol Chem 296:100037. doi: 10.1074/jbc.RA120.014793

30. Hou Y, Xue P, Bai Y, Liu D, Woods CG, Yarborough K, Fu J, Zhang Q, Sun G, Collins S, Chan JY, Yamamoto M, Andersen ME and Pi J (2012) Nuclear factor erythroid-derived factor 2-related factor 2 regulates transcription of CCAAT/enhancer-binding protein beta during adipogenesis. Free Radic Biol Med

52:462-72. doi: 10.1016/j.freeradbiomed.2011.10.453

31. Rudich A, Tirosh A, Potashnik R, Hemi R, Kanety H and Bashan N (1998) Prolonged oxidative stress impairs insulin-induced GLUT4 translocation in 3T3-L1 adipocytes. Diabetes 47:1562-9. doi: 10.2337/diabetes.47.10.1562

32. Tirosh A, Potashnik R, Bashan N and Rudich A (1999) Oxidative stress disrupts insulin-induced cellular redistribution of insulin receptor substrate-1 and phosphatidylinositol 3-kinase in 3T3-L1 adipocytes. A putative cellular mechanism for impaired protein kinase B activation and GLUT4 translocation. J Biol Chem 274:10595-602. doi: 10.1074/jbc.274.15.10595

33. Furukawa S, Fujita T, Shimabukuro M, Iwaki M, Yamada Y, Nakajima Y, Nakayama O, Makishima M, Matsuda M and Shimomura I (2004) Increased oxidative stress in obesity and its impact on metabolic syndrome. J Clin Invest 114:1752-61. doi: 10.1172/JCI21625

34. Tormos KV, Anso E, Hamanaka RB, Eisenbart J, Joseph J, Kalyanaraman B and Chandel NS (2011) Mitochondrial complex III ROS regulate adipocyte differentiation. Cell Metab 14:537-44. doi: 10.1016/j.cmet.2011.08.007

35. Yang C, Tibbitt MW, Basta L and Anseth KS (2014) Mechanical memory and dosing influence stem cell fate. Nat Mater 13:645-52. doi: 10.1038/nmat3889

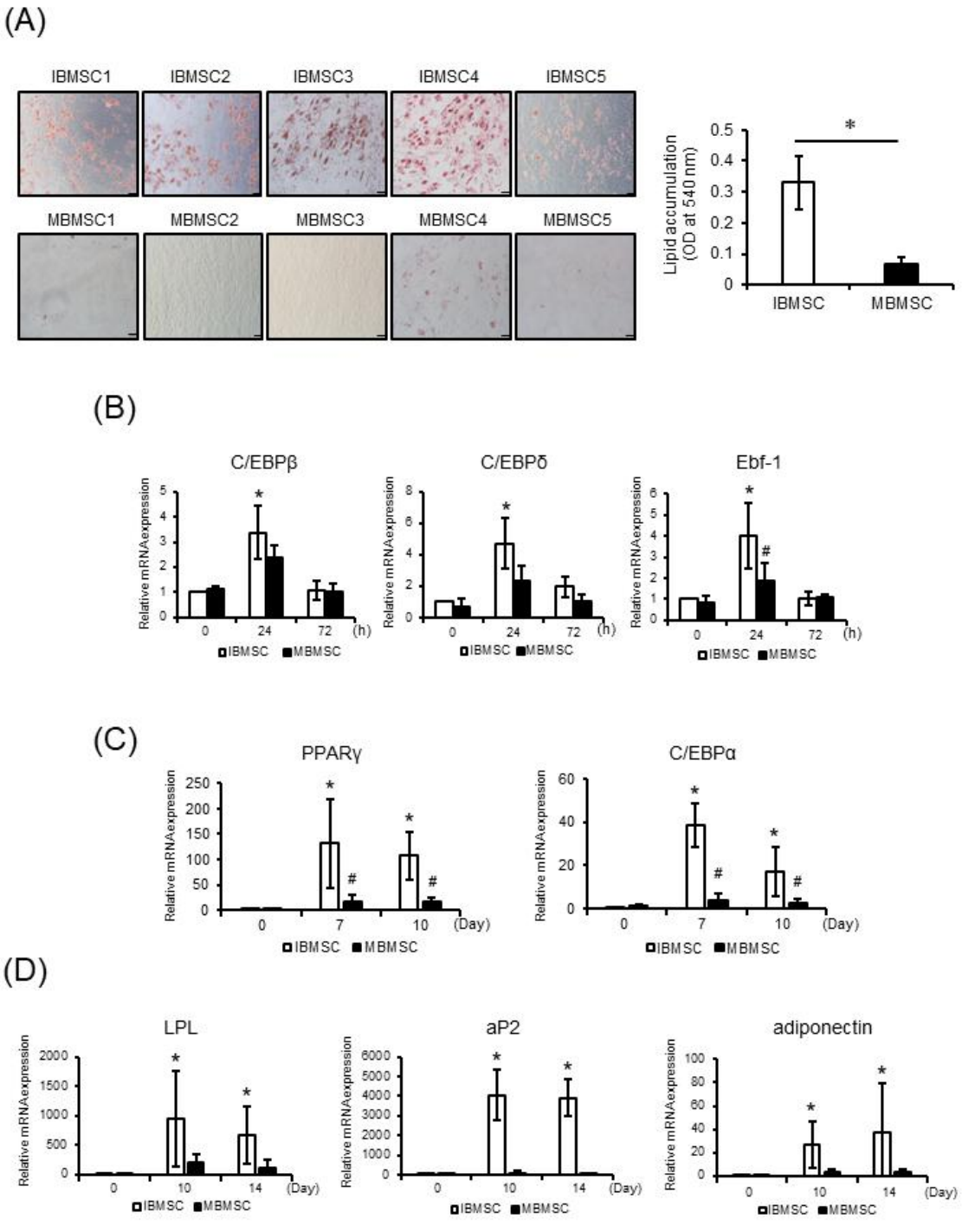
(A)
IBMSC1
IBMSC2
IBMSC3
IBMSC4
IBMSC5
MBMSC1
MBMSC2
MBMSC3
MBMSC4
MBMSC5
Lipid accumulation (OD at 540 nm)
IBMSC
MBMSC
(B)
C/EBPβ
C/EBPδ
Ebf-1
Relative mRNAexpression
(h)
IBMSC
MBMSC
(C)
PPARγ
C/EBPα
(Day)
(D)
LPL
aP2
adiponectin

Figure 1

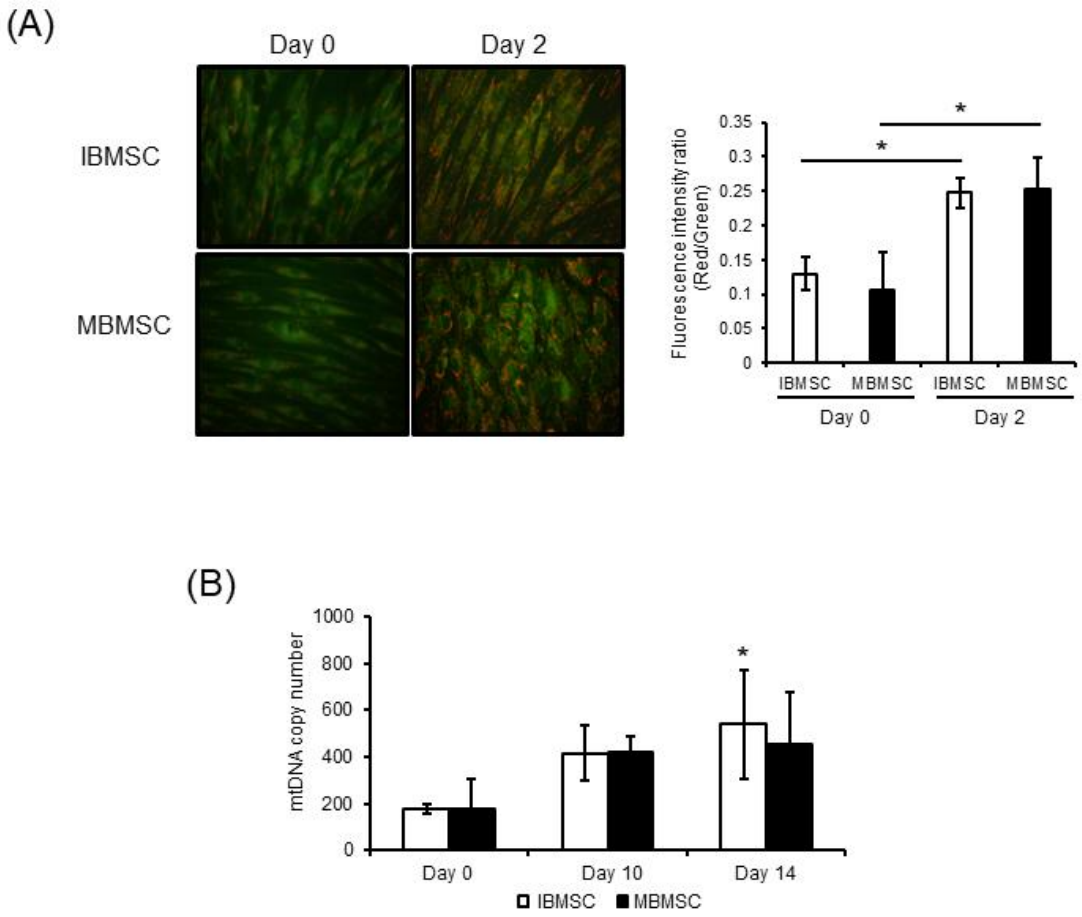
(A)
Day 0
Day 2
IBMSC
MBMSC
Fluorescence intensity ratio (Red/Green)
0.35
0.3
0.25
0.2
0.15
0.1
0.05
0
*
*
IBMSC
MBMSC
IBMSC
MBMSC
Day 0
Day 2
(B)
mtDNA copy number
1000
800
600
400
200
0
*
Day 0
Day 10
Day 14
IBMSC
MBMSC
(C)
PGC1-α
TFAM
Relative mRNA expression
100
80
60
40
20
0
*
Day 0
Day 7
IBMSC
MBMSC
Relative mRNA expression
5
4
3
2
1
0
*
Day 0
Day 7
IBMSC
MBMSC

Figure 2

(A)

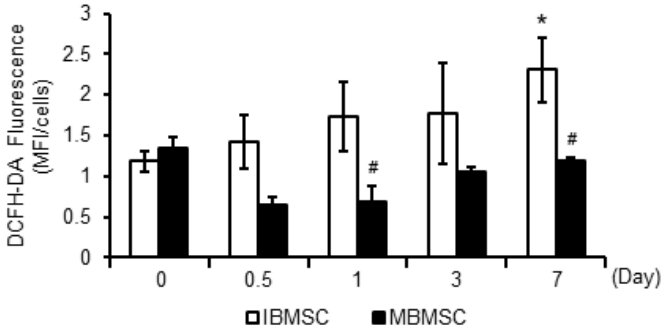
DCFH-DA Fluorescence (MFI/cells)
3
2.5
2
1.5
1
0.5
0
*
#
#
0
0.5
1
3
7
(Day)
IBMSC
MBMSC

(B)

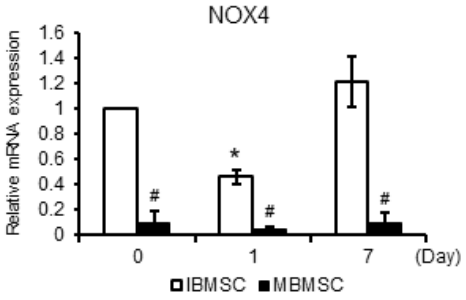
NOX4
Relative mRNA expression
1.6
1.4
1.2
1
0.8
0.6
0.4
0.2
0
*
#
#
#
0
1
7
(Day)
IBMSC
MBMSC

Figure 3

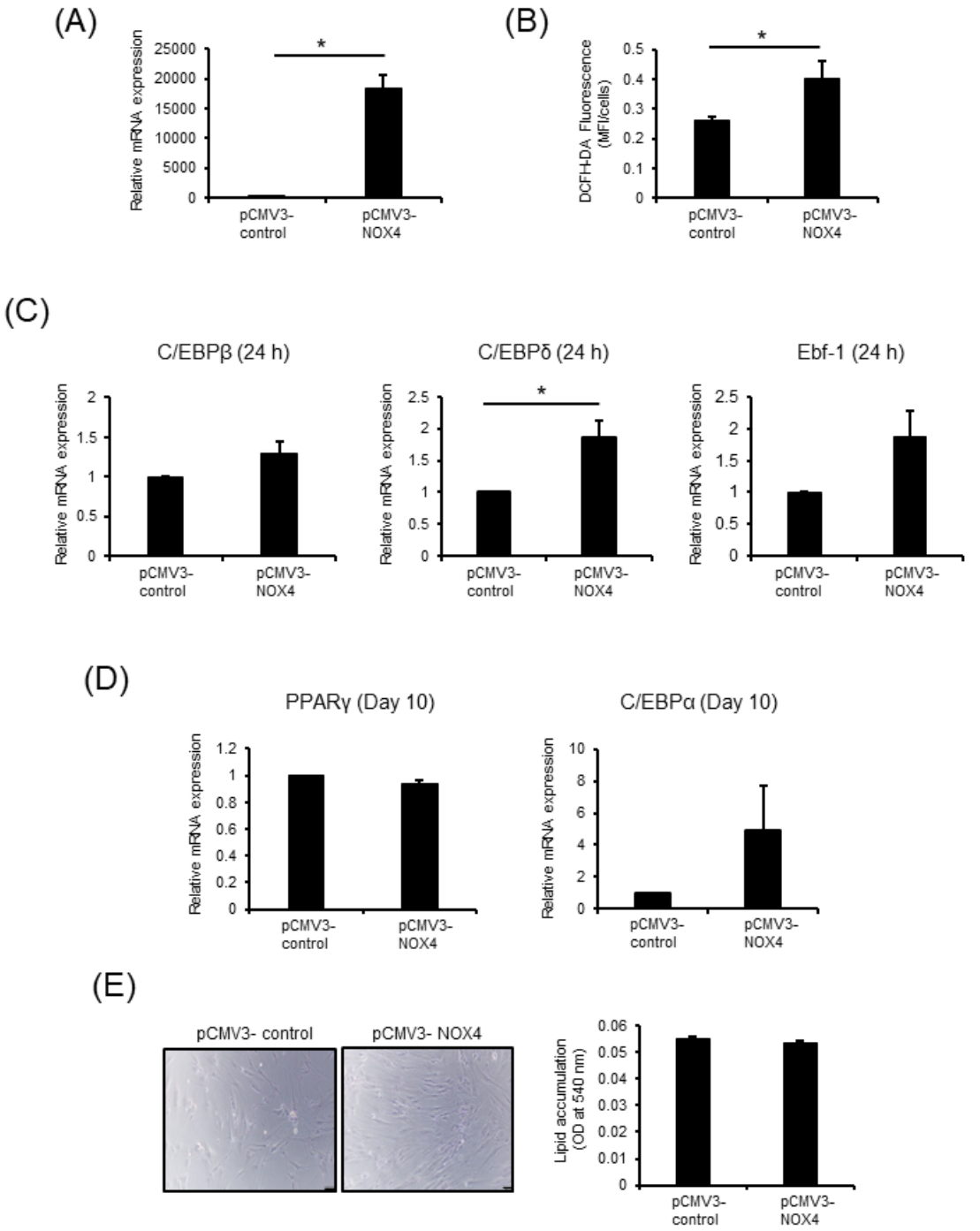
(A)
Relative mRNA expression
25000
20000
15000
10000
5000
0
*
pCMV3-control
pCMV3-NOX4
(B)
DCFH-DA Fluorescence (MFI/cells)
0.5
0.4
0.3
0.2
0.1
0
*
pCMV3-control
pCMV3-NOX4
(C)
C/EBPβ (24 h)
C/EBPδ (24 h)
Ebf-1 (24 h)
Relative mRNA expression
2
1.5
1
0.5
0
2.5
*
pCMV3-control
pCMV3-NOX4
(D)
PPARγ (Day 10)
C/EBPα (Day 10)
Relative mRNA expression
1.2
1
0.8
0.6
0.4
0.2
0
10
8
6
4
2
pCMV3-control
pCMV3-NOX4
(E)
pCMV3- control
pCMV3- NOX4
Lipid accumulation (OD at 540 nm)
0.06
0.05
0.04
0.03
0.02
0.01
0
pCMV3-control
pCMV3-NOX4

Figure 4

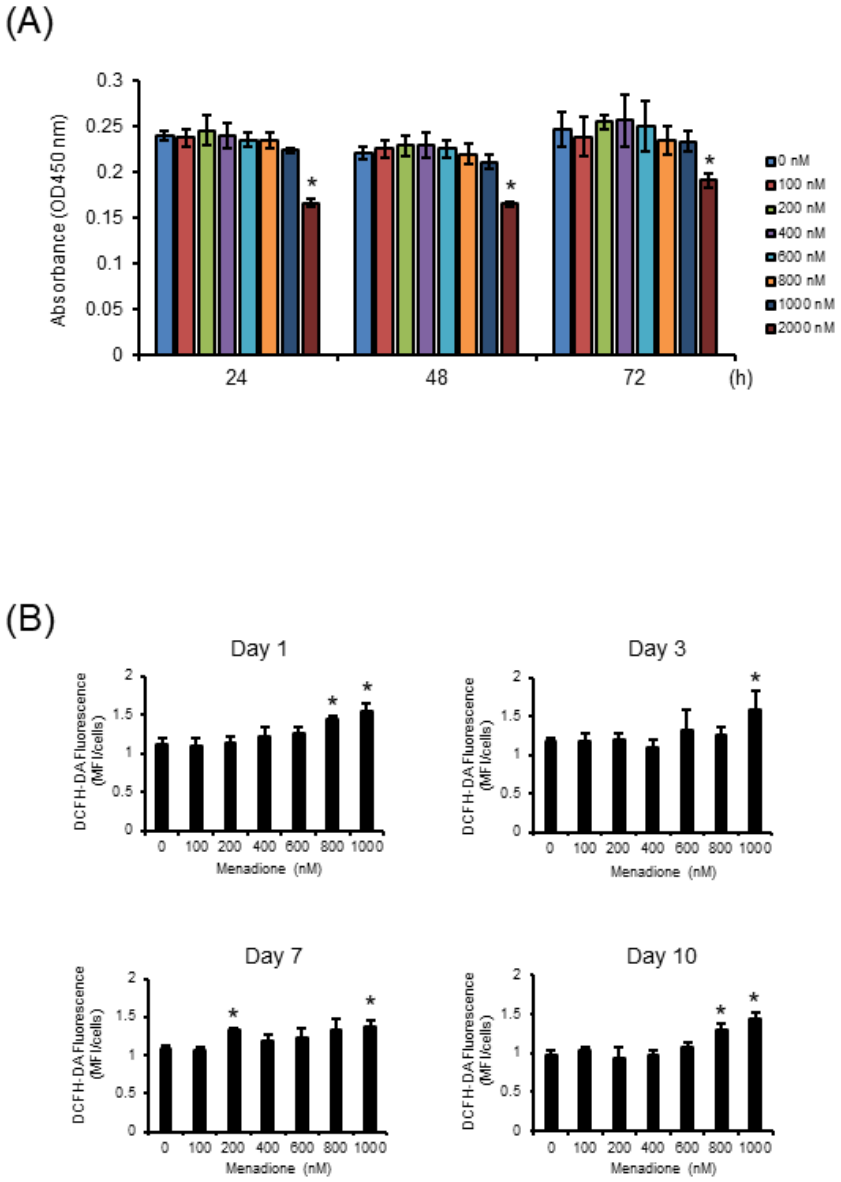
(A)
Absorbance (OD450 nm)
0.3
0.25
0.2
0.15
0.1
0.05
0
24
48
72
(h)
0 nM
100 nM
200 nM
400 nM
600 nM
800 nM
1000 nM
2000 nM
(B)
Day 1
Day 3
Day 7
Day 10
DCFH-DA Fluorescence (MFI/cells)
0 100 200 400 600 800 1000
Menadione (nM)

Figure 5

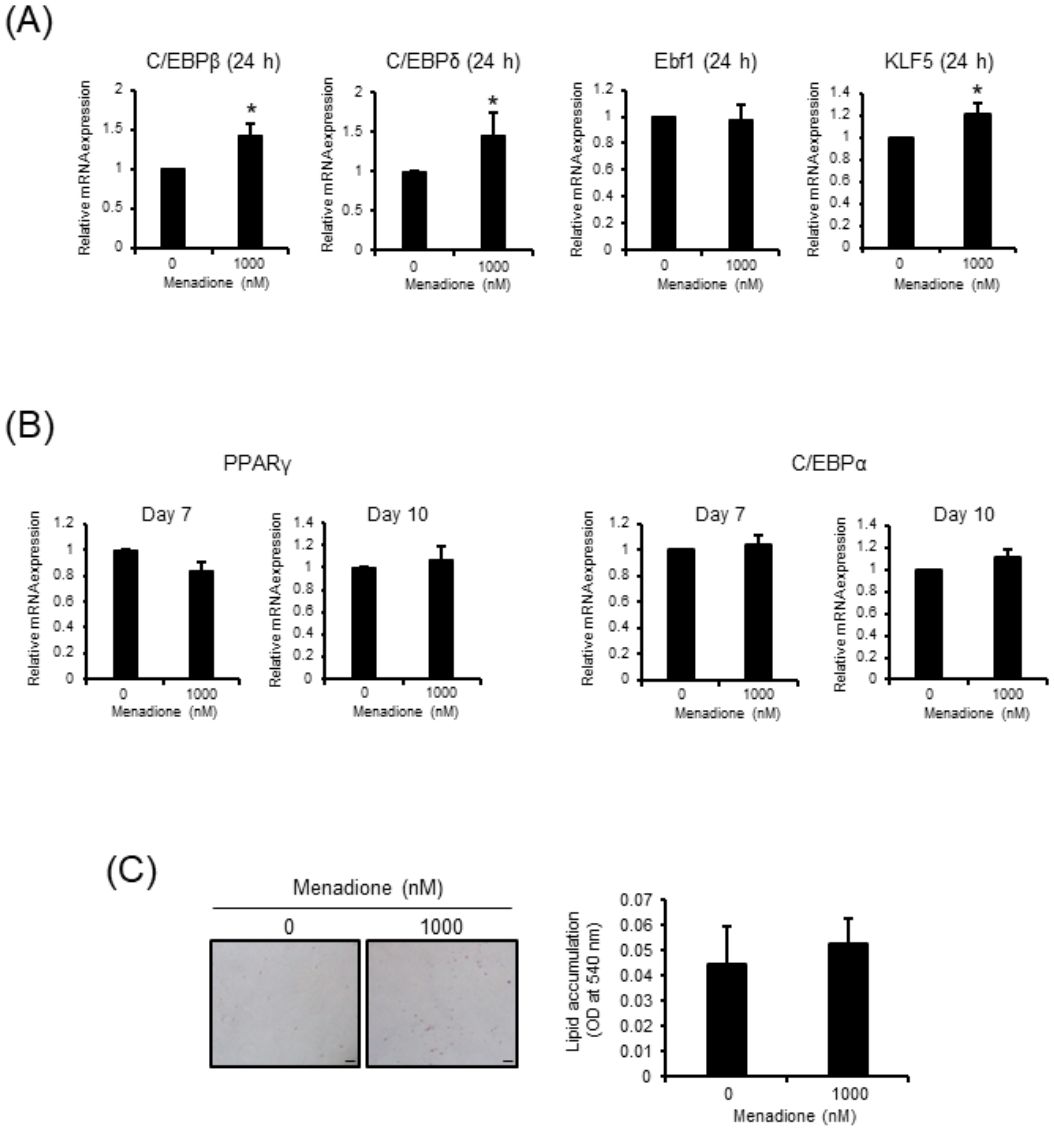
(A)
C/EBPβ (24 h)
C/EBPδ (24 h)
Ebf1 (24 h)
KLF5 (24 h)
Relative mRNAexpression
Menadione (nM)
0
1000
(B)
PPARγ
C/EBPα
Day 7
Day 10
(C)
Menadione (nM)
Lipid accumulation (OD at 540 nm)

Figure 6

Figure legends

Fig. 1. Comparison of the adipogenic potential between maxillary/mandibular bone marrow-derived mesenchymal stem cells (MBMSCs) and iliac bone marrow-derived MSCs (IBMSCs). (A) Cells were cultured in an adipogenic differentiation medium for 14 days, followed by Oil Red-O staining. The dye was extracted with 100% isopropyl alcohol, and the optical density was measured at 540 nm. Results are presented as mean ± S.D. * $p < 0.05$. Scale bar, 100 μm. mRNA expression levels of (B) C/EBPβ, C/EBPδ, and Ebf1, (C) PPARγ and C/EBPα, and (D) LPL, aP2, adiponectin in MBMSCs (n=5) and IBMSCs (n=5) cultured in adipogenic differentiation medium for the indicated times. Each gene expression was normalized to *β-actin* levels, and all data are presented as fold change compared to the IBMSCs (0 h). Results are presented as mean ± S.D. * $p < 0.05$ versus IBMSCs (0 h), $^{\#}$ $p < 0.05$ versus IBMSCs in each time point. Each experiment was repeated three times.

Fig. 2. Evaluation of mitochondrial function in maxillary/mandibular bone marrow-derived mesenchymal stem cells (MBMSCs) and iliac bone marrow-derived MSCs (IBMSCs). (A) Mitochondrial membrane potential changes induced by adipogenic differentiation were evaluated by JC-1 dye staining (red fluorescence). Mitochondrial membrane potential was assessed by the ratio of red to green fluorescence. Results are presented as mean ± S.D. * $p < 0.05$. (B) mtDNA copy number in MBMSCs (n=5) and IBMSCs

(n=5) cultured in adipogenic differentiation medium for indicated times. Results are presented as mean ± S.D. (C) mRNA expression of PGC-1α and TFAM in MBMSCs (n=5) and IBMSCs (n=5) cultured in adipogenic differentiation medium for the indicated times. PGC-1α and TFAM gene expression was normalized with β-actin levels, and data are presented as fold change compared to the IBMSCs (0 h). Results are presented as mean ± S.D. * $p < 0.05$. Each experiment was repeated three times.

Fig. 3. Intracellular reactive oxygen species (ROS) production induced by adipogenic differentiation in maxillary/mandibular bone marrow-derived mesenchymal stem cells (MBMSCs) and iliac bone marrow-derived MSCs (IBMSCs). (A) Intracellular ROS production levels were measured using DCFH-DA dye in MBMSCs (n=5) and IBMSCs (n=5). * $p < 0.05$ versus IBMSC (0 h), $^{\#}$ $p < 0.05$ versus IBMSC in each time point. (B) mRNA expression of NOX4 in MBMSCs (n=5) and IBMSCs (n=5) cultured in adipogenic differentiation medium for the indicated times. NOX4 gene expression was normalized with β-actin levels, and data are presented as fold change compared to the IBMSCs (0 h). Results are presented as mean ± S.D. * $p < 0.05$ versus IBMSC (0 h), $^{\#}$ $p < 0.05$ versus IBMSC in each time point. Each experiment was repeated three times.

Fig. 4. Effect of NOX4 overexpression on the adipogenesis of maxillary/mandibular bone marrow-derived

mesenchymal stem cells (MBMSCs). (A) Quantitative reverse transcription PCR of the relative gene expression of NOX4 in MBMSCs transfected with pCMV3 negative control (n=3) or pCMV3 NOX4 plasmids (n=3). Results are presented as mean ± S.D. * $p < 0.05$. (B) Intracellular ROS level in MBMSCs transfected with pCMV3 negative control (n=3) or pCMV3 NOX4 plasmids (n=3). The ROS level was measured using DCFH-DA dye. Results are presented as mean ± S.D. * $p < 0.05$. mRNA expression of (C) C/EBPβ, C/EBPδ and Ebf-1, and (D) PPARγ and C/EBPα in MBMSCs transfected with pCMV3 negative control (n=3) or pCMV3 NOX4 plasmids (n=3). Each gene expression was normalized to β-actin levels, and all data are presented as fold change compared to MBMSC transfected with pCMV3 negative control plasmids. Results are presented as mean ± S.D. * $p < 0.05$. (E) MBMSCs transfected with pCMV3 negative control (n=3) or pCMV3 NOX4 plasmids (n=3) were cultured in an adipogenic induction medium for 14 days, followed by Oil Red-O staining. The dye was extracted with 100 % isopropyl alcohol, and the optical density was measured at 540 nm. Results are presented as mean ± S.D. Scale bar, 100 μm.

Fig. 5. Intracellular reactive oxygen species (ROS) production induced by menadione in maxillary/mandibular bone marrow-derived mesenchymal stem cells (MBMSCs). (A) Effect of menadione on MBMSC viability. MBMSCs were treated with menadione (100–2000 nM) or the vehicle (dimethyl sulfoxide: DMSO) for 24–72 h, and the cytotoxic effect was then evaluated by WST-1 assay (n=3). Results

are presented as mean ± S.D. * $p < 0.05$ versus 0 nM at each time point. (B) MBMSCs were cultured for 1, 3, 7, and 10 days in an adipogenic induction medium containing menadione (100–1000 nM) or the vehicle (dimethyl sulfoxide: DMSO). Intracellular ROS production levels were measured using DCFH-DA dye in MBMSCs (n=3). Results are presented as mean ± S.D. * $p < 0.05$ versus 0 nM at each time point.

Fig. 6. Involvement of reactive oxygen species (ROS) production by menadione in the adipogenic differentiation of maxillary/mandibular bone marrow-derived mesenchymal stem cells (MBMSCs). Gene expression of (A) C/EBPβ, C/EBPδ, and Ebf-1 and (B) PPARγ and C/EBPα in MBMSCs cultured for the indicated times in adipogenic induction medium containing menadione (1000 nM) or the vehicle (dimethyl sulfoxide: DMSO). Each gene expression was normalized with β-actin expression levels, and data are presented as fold change compared to 0 nM. Results are presented as mean ± S.D. * $p < 0.05$. (C) MBMSCs were cultured in an adipogenic differentiation medium containing menadione (1000 nM) or the vehicle (dimethyl sulfoxide: DMSO) for 14 days, followed by Oil Red-O staining. The dye was extracted with 100% isopropyl alcohol, and the optical density was measured at 540 nm. Scale bar, 100 μm.